Modelling and offset-free predictive control of the parallel-type double inverted pendulum

Paul, Ager; Kucukdemiral, ibrahim Beklan; Bevan, Geraint

Published in:
2022 10th International Conference on Systems and Control (ICSC)

DOI:
10.1109/ICSC57768.2022.9993951

Publication date:
2023

Document Version
Author accepted manuscript

Modelling and Offset-free Predictive Control of the Parallel-Type Double Inverted Pendulum*

Ager Paul[1], Ibrahim Küçükdemiral[1] and Gerain Bevan[1]

***Abstract*— This paper presents a nonlinear model of the parallel-type double inverted pendulum system with an elastic spring that produces opposing torques on the pendulums. The effects of solid and viscous frictional forces are considered in the developed model. The stabilising control of the nonlinear system is investigated by designing an offset-free model predictive control (OfMPC) scheme based on the linearised model. The use of OfMPC makes it possible to optimize the system performance while also ensuring that the physical limits of the system are not exceeded. Numerical simulation is used to show the effectiveness and prospective benefits of using the proposed controller over the conventional method.**

I. INTRODUCTION

The inverted pendulum on a cart system refers to a mechanical system that consists of a pendulum that is attached through a flexible link to a freely moving cart along a horizontal plane. In control theory and its applications, the inverted pendulum on a cart problem is well-known and have been widely studied [1], [2], [3]. The system is usually used as a benchmark for testing controllers since it represents a typical multivariable, nonlinear and unstable system. Moreover, the inverted pendulum system provides adequate models used to represent a significant number of technical problems in robotics [4]. As discussed in [5], the inverted pendulum system has been used as representative models in the launching of a rocket [6], the motion of a robot [7], [8] and the movement of an hexapod robot [9].

The parallel-type double inverted pendulum system refers to two single inverted pendulums placed side by side. In such a system, the main aim is to simultaneously control the two pendulums. Different versions of the system exist. The first version comprises two pendulums both connected via a flexible link to a single cart. The modelling including those considering the friction between different parts and control of this type of pendulum has been widely studied [10], [11], [12].

The second form of the parallel-type double inverted pendulum system comprises two pendulums usually of equal lengths that are hinged through a flexible link on two different carts. Two variants of this particular form of the system have been presented in the literature. In the one described in [13], there is no interaction between the two pendulums. A more technically challenging version [14] has an elastic spring connecting the two pendulums which lead to interactions between the pendulums. However, the mathematical model of the parallel-type double inverted pendulum system presented in [14] neglected the friction forces between the horizontal axis and the rollers of the cart and that between the hinge and the pendulums. Moreover, they [14] only considered a linear model even though the system is highly nonlinear. In addition, they failed to consider the physical limits of the system which can potentially affect the controller's performance.

Therefore, this paper presents a more detailed mathematical model with the solid and viscous frictional forces which where not considered in [3]. Although the linearised version of the model is used to design a controller to achieve stabilising control, it is tested on the nonlinear model. Furthermore, this paper proposes the use of model predictive control (MPC), for the first time, to stabilise this system as previous studies [13], [14] employed linear quadratic regulator. In [15], it was explained that traditional controllers such as PID and LQR where saturation blocks are used to implement constraints on the system can generally provide higher oscillations when input saturation occurs. This is primarily due to the fact that the control command planning does not consider the constraints. MPC, on the other hand, provides a natural way of incorporating constraints into the controller [16], [17] because the constraints are included in the optimisation problem to be solved online in each sampling instant.

Furthermore, to address the challenge of offset which may be caused by the model mismatch between the actual model and the linearized version used in the controller design, offset-free MPC (OfMPC) is used in this work. To design OfMPC, two approaches have been widely used [18], [19] - the disturbance model and the velocity model methods. In this paper, the velocity model approach would be used as it has been shown [19] that it can provide less sensitivity to measurement noise which is almost unavoidable in real applications.

The rest of this paper is organised as follows. Section II presents the description and mathematical modelling of the system based on Lagrange equations. In Section III, the design of the OfMPC scheme is presented while Section IV provides a simulation study where results for both the full-state feedback controller and the observer-based OfMPC are presented. Section V presents discussions of the results from the numerical simulation while Section VI provides the conclusions.

*This work was not supported by any organization

[1]The authors are with the Department of Applied Science, School of Computing, Engineering and Built Environment, Glasgow Caledonian University, 70 Cowcaddens Rd, G4 0BA, Glasgow, UK. Emails: pager200@caledonian.ac.uk, iku1@gcu.ac.uk, geraint.bevan@gcu.ac.uk.

II. Modelling of the Dynamical System

The physical system illustrated in Figure 1 shows that the system comprises two carts, two straight slide rails, two pendulums and each cart is driven by electric motor units, M. The voltages applied via the DC motor to provide a desired motion of the carts are denoted as the controls u_1 and u_2. The pendulums are hinged on the centre of the carts O_1 and O_2 with the ability to rotate through the vertical plane. It is important to note that both carts can move back and forth on the rails. The parameters needed to derive the mathematical model of the system are shown on the schematic diagram in Figure 1. To model the system, the

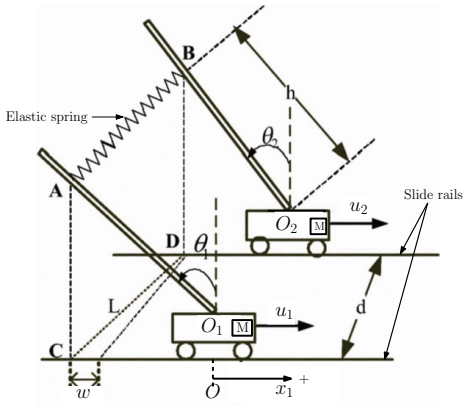

Fig. 1. Schematic diagram showing the parameters of the parallel-type double inverted pendulum. Adapted from [20].

effect of solid friction between the carts of masses M_1 and M_2 and the slide rails are considered with coefficient denoted by μ_1 and μ_2; the viscous frictional coefficients v_1 and v_2 at the pivot points connecting the pendulums of masses m_1 and m_2 to the carts is also considered. The length of pendulums 1 and 2 are respectively denoted as l_1 and l_2. Furthermore, the moment of inertia of the pendulum 1 is J_1 while that of the second pendulum is J_2. Although Xing et *al.* [20] neglected the effect of both viscous and solid frictions in modelling the system, this paper considers them as they are usually important in real systems. Moreover, the nonlinear model of the system is used in the simulation to give a good approximation of the actual physical system.

The displacement of the carts from the centre points O, is denoted x_1 and x_2 for cart 1 and cart 2, respectively. This displacement is positive if it is towards the right direction. In Figure 1, the angular displacements θ_1 and θ_2 are positive in the clockwise direction. The parameter w, is denoted as the difference between the projection of points **A** and **B** on the horizontal plane. The definition of all the parameters and their values needed to describe the system are presented in Table I. To model the parallel type-double inverted pendulum, Lagrange approach is used as follows:

$$L = T(\dot{q}, q) - V(q) \tag{1}$$

$$\frac{d}{dt}\left(\frac{\partial L}{\partial \dot{q}_i}\right) - \frac{\partial L}{\partial q_i} = Q_i, \ i = 1, 2, \ \ldots \ n. \tag{2}$$

TABLE I

Parameters describing the parallel-type double inverted pendulum

Notation	Meaning of Parameter	Value
l_1, l_2	Length of pendulum 1 and the pendulum 2 from pivot to the centre of mass	0.25m
m_1, m_2	Mass of pendulum 1 and pendulum 2.	0.109kg
M_1, M_2	Mass of cart 1 and cart 2	1.096kg
x_1, x_2	Displacement of cart 1 and 2 from the centre point O	-1m to +1m
d	Distance between the slide rails	0.187m
h	length from spring endpoint A and B to pivot O_2 and O_2	0.4m
k_s	Elastic spring constant	24.5Nm^{-1}
g	Acceleration due to gravity	9.81ms^{-2}
J_1, J_2	Moment of inertia of pendulum 1 and 2	9.083mkgm^2
l_o	Original length of the spring	0.181m
μ_1, μ_2	Solid friction constants	0.002
v_1, v_2	Viscous friction constants	0.001

where L is the Lagrangian operator, T is the kinetic energy and V is the potential energy of the system. The variable q_i is the vector of generalised coordinate or degree of freedom of the double inverted system; Q_i represents the vector of external forces acting on the system, with i representing the displacements of the two carts and the angular displacement of the two pendulums.

The energy of the system can be modelled as follows [21], [5]:

Cart 1:
potential energy (PE): $V_{M_1} = 0$;
Kinetic energy (KE): $T_{M_1} = \frac{1}{2} M_1 \dot{x}_1^2$.

Cart 2:
PE: $V_{M_2} = 0.$; KE: $T_{M_2} = \frac{1}{2} M_2 \dot{x}_2^2$.

Pendulum 1:
PE: $V_{m_1} = m_1 g l_1 \cos\theta_1$;
KE: $T_{m_1} = \frac{1}{2} J_1 \dot{\theta}_1^2 + \frac{1}{2} m_1 \{ \left[\frac{d}{dt}(l_1 \cos\theta_1)\right]^2 + \left[\frac{d}{dt}(x_1 - l_1 \sin\theta_1)\right]^2 \}$

Pendulum 2:
PE: $V_{m_2} = m_2 g l_2 \cos\theta_2$
KE: $T_{m_2} = \frac{1}{2} J_2 \dot{\theta}_2^2 + \frac{1}{2} m_2 \{ \left[\frac{d}{dt}(l_2 \cos\theta_2)\right]^2 + \left[\frac{d}{dt}(x_2 - l_2 \sin\theta_2)\right]^2 \}$
where the moment of inertia of the pendulums are $J_1 = \frac{4}{3} m_1 l_1^2$ and $J_2 = \frac{4}{3} m_2 l_2^2$

Elastic spring:
PE: $V_{spring} = \frac{1}{2} k_s (l_d - l_o)^2$
where l_o is the unstrained length of the spring and l_d is the length of the draught spring.

Based on the above equations, the total potential and kinetic energy of the parallel-type double inverted pendulum system can be given as follows:

$$T = T_{m_1} + T_{m_2} + T_{M_1} + T_{M_2} \tag{3}$$

$$V = V_{m_1} + V_{m_2} + V_{M_1} + V_{M_2} + V_{spring} \tag{4}$$

By substituting (3) and (4) into (1), one obtains:

$$
\begin{aligned}
L =& \frac{1}{2}M_1\dot{x}_1^2 + \frac{1}{2}M_2\dot{x}_2^2 + \frac{1}{2}J_1\dot{\theta}_1^2 + \frac{1}{2}J_2\dot{\theta}_2^2 + \\
& \frac{1}{2}m_1\left(\dot{x}_1^2 - 2\dot{x}_1 l_1\dot{\theta}_1\cos\theta_1 + l_1^2\dot{\theta}_1^2\right) \\
& + \frac{1}{2}m_2\left(\dot{x}_2^2 - 2\dot{x}_2 l_2\dot{\theta}_2\cos\theta_2 + l_2^2\dot{\theta}_2^2\right) - \\
& m_1 g l_1\cos\theta_1 - m_2 g l_2\cos\theta_2 - \frac{1}{2}k_s(l_d - l_o)^2
\end{aligned} \tag{5}
$$

The equation of motion of the parallel-type double inverted pendulum system can be obtained from the partial differential equation (2) as follows:

$$
\frac{d}{dt}\left(\frac{\partial L}{\partial \dot{x}_1}\right) - \frac{\partial L}{\partial x_1} = u_1 - f_{r_1}, \tag{6}
$$

$$
\frac{d}{dt}\left(\frac{\partial L}{\partial \dot{x}_2}\right) - \frac{\partial L}{\partial x_2} = u_2 - f_{r_2}, \tag{7}
$$

$$
\frac{d}{dt}\left(\frac{\partial L}{\partial \dot{\theta}_1}\right) - \frac{\partial L}{\partial \theta_1} = -f_{v_1}, \tag{8}
$$

$$
\frac{d}{dt}\left(\frac{\partial L}{\partial \dot{\theta}_2}\right) - \frac{\partial L}{\partial \theta_2} = -f_{v_2}, \tag{9}
$$

where u_1 and u_2 is the voltage (V) applied to cart 1 and 2 via the motor to move the carts; f_{r_1} and f_{r_2} are the solid frictional forces between the cart 1nd cart 2 and the horizontal plane; f_{v_1} and f_{v_2} are the corresponding viscous frictional forces at the pivot points of the pendulums. These forces can be modelled as follows [5], [11]:

$$
f_{r_1} = \mu_1\dot{x}_1, f_{r_2} = \mu_2\dot{x}_2, f_{v_1} = v_1\dot{\theta}_1, f_{v_2} = v_2\dot{\theta}_2. \tag{10}
$$

For convenience in the derivation of the equations of motion for the system in Figure (1), let $j = 1, 2$. By expanding and simplifying Equations (6), (7), (8) and (9), the following equations can then be obtained:

$$
\begin{aligned}
(M_j + m_j)\ddot{x}_j - m_j l_j\ddot{\theta}_j\cos\theta_j + m_j l_j\dot{\theta}_j^2\sin\theta_j \\
+ \frac{1}{2}k_s\frac{\partial}{\partial x_j}\left[(l_d - l_o)^2\right] = F_j - \mu_j\dot{x}_j
\end{aligned} \tag{11}
$$

$$
\begin{aligned}
\frac{7}{3}m_j l_j^2\ddot{\theta}_j - m_j l_j\ddot{x}_j\cos\theta_j - m_j g l_j\sin\theta_j \\
+ \frac{1}{2}k_s\frac{\partial}{\partial \theta_j}\left[(l_d - l_o)^2\right] = -v_j\dot{\theta}_j
\end{aligned} \tag{12}
$$

where $l_d = \sqrt{d^2 + w^2}$ and $w = (x_2 - h\sin\theta_2) - (x_1 - h\sin\theta_1)$ is the distance between the projections C and D along the direction of the trails shown in Figure 1. The derivatives: $\frac{\partial}{\partial x_j}\left[(l_d - l_o)^2\right]$ and $\frac{\partial}{\partial \theta_j}\left[(l_d - l_o)^2\right]$ can be shown to be given as follows:

$$
\begin{aligned}
\frac{\partial}{\partial x_1}\left[(l_d - l_o)^2\right] =& -2\left(1 - \frac{l_o}{l_d}\right)(x_2 - x_1 \\
& - h(\sin\theta_2 + \sin\theta_1))
\end{aligned} \tag{13}
$$

$$
\frac{\partial}{\partial x_2}\left[(l_d - l_o)^2\right] = 2\left(1 - \frac{l_o}{l_d}\right)(x_2 - x_1 - h\sin\theta_2 + h\sin\theta_1) \tag{14}
$$

$$
\begin{aligned}
\frac{\partial}{\partial \theta_1}\left[(l_d - l_o)^2\right] =& 2\left(1 - \frac{l_o}{l_d}\right)(x_2 - x_1 - h\sin\theta_2 \\
& + h\sin\theta_1)(h\cos\theta_1)
\end{aligned} \tag{15}
$$

$$
\begin{aligned}
\frac{\partial}{\partial \theta_2}\left[(l_d - l_o)^2\right] =& 2\left(1 - \frac{l_o}{l_d}\right)(x_2 - x_1 - h\sin\theta_2 \\
& + h\sin\theta_1)(-h\cos\theta_2)
\end{aligned} \tag{16}
$$

By substituting (13) - (16) into (11) and (12), the non-linear model describing the motion of the dynamical parallel-type double inverted pendulum system in Figure 1 can be expressed more elegantly as follows:

$$
\mathbf{M}(q)\ddot{q} + \mathbf{C}(q, \dot{q})\dot{q} + \mathbf{K}(q) = Hu \tag{17}
$$

where

$$
\mathbf{M} = \begin{bmatrix} M_1+m_1 & -m_1 l_1\cos\theta_1 & 0 & 0 \\ -m_1 l_1\cos\theta_1 & \frac{7}{3}m_1 l_1^2 & 0 & 0 \\ 0 & 0 & M_2+m_2 & -m_2 l_2\cos\theta_2 \\ 0 & 0 & -m_2 l_2\cos\theta_2 & \frac{7}{3}m_2 l_2^2 \end{bmatrix}
$$

$$
\mathbf{C} = \begin{bmatrix} \mu_1 & m_1 l_1\dot{\theta}_1\sin\theta_1 & 0 & 0 \\ 0 & v_1 & 0 & 0 \\ 0 & 0 & \mu_2 & m_2 l_2\dot{\theta}_2\sin\theta_2 \\ 0 & 0 & 0 & v_2 \end{bmatrix}
$$

$$
\mathbf{K} = \begin{bmatrix} K_1 \\ K_2 - m_1 g l_1\sin\theta_1 \\ K_3 \\ K_4 - m_2 g l_2\sin\theta_2 \end{bmatrix}, \; H = \begin{bmatrix} 1 & 0 \\ 0 & 0 \\ 0 & 1 \\ 0 & 0 \end{bmatrix}
$$

where $K_1 = -k_s\left(1 - \frac{l_o}{l_d}\right)(x_2 - x_1 - h\sin\theta_2 + h\sin\theta_1)$, $K_2 = -hK_1\cos\theta_1$, $K_3 = -K_1$, $K_4 = hK_1\cos\theta_2$ and $u = [u_1\ u_2]^T$. By defining $x = [q\ \dot{q}]^T = [x_1\ \theta_1\ x_2\ \theta_2\ \dot{x}_1\ \dot{\theta}_1\ \dot{x}_2\ \dot{\theta}_2]^T$ as the state vector, Equation (17) can be written the non-linear model of the form:

$$
g(x, u) = \begin{bmatrix} \dot{q} \\ M^{-1}(Hu - C\dot{q} - K) \end{bmatrix}. \tag{18}
$$

III. Optimal Control Design

In this section, the design of discrete-time linear quadratic regulator and model-based predictive control which would be employed for the control of the non-linear model (18) would be presented. we first present the linearization of the non-linear model in the following section.

A. Linearisation of Dynamical System

Since this paper aims to study the stabilisation of the two pendulums in the vicinity of the upward position, the linearisation is is carried out around the vertical pendulums positions. Therefore, the balance point for linearisation is given as $\theta_1 \approx 0$ and $\theta_2 \approx 0$. Also, it is assumed that the balance point for the two carts on the trails are the central points where $x_1 = 0$ and $x_2 = 0$. To linearise the system around this equilibrium points, the following approximations hold: $\sin\theta_1 = \theta_1$, $\sin\theta_2 = \theta_2$, $\cos\theta_1 = \cos\theta_2 = 1$, $\dot{\theta}_1^2 = \dot{\theta}_2^2 = 0$. Based on the defined approximations needed to linearise the system, the models (18) can be transformed into the state-space model of the form:

$$
\begin{aligned}
\dot{x} &= Ax + Bu, \\
y &= Cx
\end{aligned} \tag{19}
$$

where $x \in \mathbb{R}^n, u \in \mathbb{R}^m, y \in \mathbb{R}^p$, $A \in \mathbb{R}^{n\times n}$ is the system matrix, $B \in \mathbb{R}^{n\times m}$ is the control matrix, $C \in \mathbb{R}^{p\times n}$ is the output matrix. More specifically, the state-space model matrices are give as follows:

$$A = \begin{bmatrix} 0 & I \\ -M(0)^{-1}\frac{\partial K}{\partial x} & -M(0)^{-1}C(0) \end{bmatrix},\ B = \begin{bmatrix} 0 \\ -M(0)^{-1}H \end{bmatrix}$$

By defining $\beta = -k_s\left(1 - \frac{l_o}{l_d}\right)$, the conditions of linearisation described previously imply that

$$K = \begin{bmatrix} -\beta h\theta_2 + \beta h\theta_1 \\ \beta h^2\theta_2 - \beta h^2\theta_1 + m_1 g l_1 \\ \beta h\theta_2 - \beta h\theta_1 \\ -\beta h^2\theta_2 + \beta h^2\theta_1 + m_2 g l_2 \end{bmatrix},$$

$$\frac{\partial K}{\partial x} = \begin{bmatrix} 0 & \beta h & 0 & -\beta h \\ 0 & -\beta h^2 & 0 & \beta h^2 \\ 0 & -\beta h & 0 & \beta h \\ 0 & \beta h^2 & 0 & -\beta h^2 \end{bmatrix}$$

By sustituting the parameters of the dynamic system shown in Table I into (19), the following system matrices are obtained for the parallel-type double inverted pendulum:

$$A = \begin{bmatrix} 0 & 0 & 0 & 0 & 1 & 0 & 0 & 0 \\ 0 & 0 & 0 & 0 & 0 & 1 & 0 & 0 \\ 0 & 0 & 0 & 0 & 0 & 0 & 1 & 0 \\ 0 & 0 & 0 & 0 & 0 & 0 & 0 & 1 \\ -0.21 & 0.48 & 0.21 & -0.085 & -0.0013 & -0.0013 & 0 & 0 \\ 19.42 & 9.7113 & -19.42 & 7.77 & -0.0022 & -0.0589 & 0 & 0 \\ 0.21 & -0.085 & -0.21 & 0.48 & 0 & 0 & -0.0013 & -0.0013 \\ -19.42 & 7.77 & 19.42 & 9.71 & 0 & 0 & -0.0022 & -0.059 \end{bmatrix}$$

$$B = \begin{bmatrix} 0 & 0 \\ 0 & 0 \\ 0 & 0 \\ 0 & 0 \\ 0.8633 & 0 \\ 1.4800 & 0 \\ 0 & 0.8633 \\ 0 & 1.4800 \end{bmatrix},\ C = \begin{bmatrix} 1 & 0 & 0 & 0 & 0 & 0 & 0 & 0 \\ 0 & 1 & 0 & 0 & 0 & 0 & 0 & 0 \\ 0 & 0 & 1 & 0 & 0 & 0 & 0 & 0 \\ 0 & 0 & 0 & 1 & 0 & 0 & 0 & 0 \end{bmatrix}$$

B. MPC Design

The design of MPC can be carried out such that the physical constraint on the parallel-type double inverted pendulum as well as modelling errors can be addressed through online optimisation. This paper uses the approach described in [22], [19] where the velocity model of the plant is used to develop an OfMPC to eliminate modelling errors and other system uncertainties. Since the algorithm may need to be implemented using a digital processing unit in practice, it is necessary to obtain the discretised version of the model (19) as follows:

$$\begin{aligned} x(k) =& A_d x(k) + B_d u(k), \\ y(k) =& C_d x(k) \end{aligned} \tag{20}$$

where k is the discrete step at time kT_s, where T_s is the sampling time. With regards to addressing relatively slowly-varying modelling uncertainties and external disturbance (such as wind gust whose effect on the carts may not be negligible), the use of velocity model has been shown to be an effective approach [23], [24]:

$$\begin{aligned} \tilde{x}(k) =& \tilde{A}\tilde{x}(k) + \tilde{B}\Delta u(k) \\ y(k) =& \tilde{C}\tilde{x}(k) \end{aligned} \tag{21}$$

where $\Delta u(k) = u(k) - u(k-1)$ is the control increment, $x(k) = \begin{bmatrix} x(k) - x(k-1) \\ y(k-1) \end{bmatrix}$ is the state increment and the augmented matrices are defined explicitly as

$$\tilde{A} = \begin{bmatrix} A_d & 0 \\ C_d & I \end{bmatrix},\ \tilde{B} = \begin{bmatrix} B_d \\ 0 \end{bmatrix},\ \tilde{C} = \begin{bmatrix} C_d & I \end{bmatrix}.$$

To compute the control input $u(k)$ in every time step, the following optimisation problem needs to be solved in every time step:

$$\begin{aligned} J(k) = \frac{1}{2}\parallel e(k+N)\parallel_S^2 + \frac{1}{2}\sum_{i=0}^{N-1}\parallel e(k+i)\parallel_Q^2 \\ + \frac{1}{2}\sum_{j=0}^{N_u-1}\parallel \Delta u(k+j)\parallel_R^2 \end{aligned} \tag{22}$$

subject to:

$$|u(k+j)| \le u_{\max},\ |x_j(k+i)| \le x_{\max}$$

The constraints $u_{\max}$ denotes the maximum input voltage that can be applied to the carts through a DC motor; the constraints on the two carts position denoted x_j is due to the fact that the carts are restricted to move through $\pm$1m distance on the rails For details on derivation of the constraints inequalities using the velocity form of MPC, refer to [23]. Furthermore, N is the prediction horizon, $e(k) = \bar{y}(k) - y(k)$, where $\bar{y}(k)$ denote the output reference. The matrices S and Q are positive semi-definite while R is a positive definite matrix. The terminal cost $e(k+N)$ is used to ensure nominal stability of the closed-loop system provided that the weight S is chosen such that $S = Q + ASA - (ASB)(R + B^TSB)^{-1}B^TSA$ [25], [15].

By defining the optimisation variable $z = [\Delta u(k), \Delta u(k+1), \dots \Delta u(N-1)]^T$, the quadratic optimisation problem (22) can be used transformed into:

$$z^* = \text{argmin}\ \frac{1}{2}z^THz + \begin{bmatrix}\tilde{x}^T & \bar{y}^T\end{bmatrix}Fz \tag{23}$$

subject to:

$$\Gamma z \le \gamma$$

where Γ and γ represent a matrix and vector used to apply the necessary limit on the carts positions and the input forces. The Hessian matrix H can be calculate offline while F should be computed online in every time step. These matrices are given as:

$$H = \bar{B}\bar{Q}\bar{B} + \bar{R},\ F = \begin{bmatrix}\bar{A}\bar{Q}\bar{B} \\ -\bar{T}\bar{B}\end{bmatrix}$$

$$\bar{B} = \begin{bmatrix} \tilde{B} & 0 & \cdots & 0 \\ \tilde{A}\tilde{B} & \tilde{B} & \cdots & 0 \\ \vdots & \vdots & \ddots & \vdots \\ \tilde{A}^{N-1}\tilde{B} & \tilde{A}^{N-2}\tilde{B} & \cdots & \tilde{A}^{N-N_u}\tilde{B} \end{bmatrix}, \bar{T} = \begin{bmatrix} Q\tilde{C} & \cdots & 0 & 0 \\ \vdots & \ddots & \vdots & \\ 0 & \cdots & Q\tilde{C} & 0 \\ 0 & \cdots & 0 & S\tilde{C} \end{bmatrix}$$

$$\bar{A} = \begin{bmatrix} \tilde{A} \\ \tilde{A}^2 \\ \vdots \\ \tilde{A}^N \end{bmatrix}, \bar{Q} = \begin{bmatrix} \tilde{C}^TQ\tilde{C} & \cdots & 0 & 0 \\ \vdots & \ddots & \vdots & \\ 0 & \cdots & \tilde{C}^TQ\tilde{C} & 0 \\ 0 & \cdots & 0 & \tilde{C}^TS\tilde{C} \end{bmatrix}$$

amd $\bar{R} = \texttt{diag}([R, \dots, R])$. Based on the computed optimal solution z^*, the receding horizon principle can be used to obtain the control increment in every time step as

$\Delta u^*(k) = [I_m\ 0]z^*$ from which the optimal control input u^* to be applied to the nonlinear model (17) can be calculated as

$$u^*(k) = \Delta u^*(k) + u(k-1) \tag{24}$$

where $u(k-1)$ is the previous control input.

IV. Numerical Simulation

In this section, the MPC designed using the linear model (20) would be investigated in terms of its suitability for the control of the continuous time nonlinear model (18). To implement the OfMPC, the continuous-time system is sampled at a sampling period of, $T_s = 0.05$ s, prediction horizon is chosen as $N = 10$ and the control horizon $N_u = 3$. Furthermore, $Q = S = \texttt{blkdiag}(1.5, 0.1, 1.5, 0.1)$ and $R = \texttt{blkdiag}(0.05, 0.05)$. The optimisation problem (23) is solved using `quadprog` in MATLAB in the implementation of the controller.

A. Full-State Feedback Control

In this case, the OfMPC is employed to control the two pendulum system under the assumption that all the states of the system are measurable. Firstly, an initial condition of the system denoted $\bar{x} = [0.01, 0, 0.015, 0, 0, 0, 0, 0]^T$ is used and this means that the two carts deviate from their equilibrium position (0m) with 0.01m and 0.015m for carts 1 and 2, respectively. The input voltages that can be applied by either DC motor in cart 1 and 2 is constrained to $u_j = \pm 5$V while the cart positions are constrained using $x_j = \pm 1$m. The output results obtained in controlling the nonlinear system are shown in Figure 2 while the control voltage signal is shown in Figure 3. A more challenging initial conditions where the

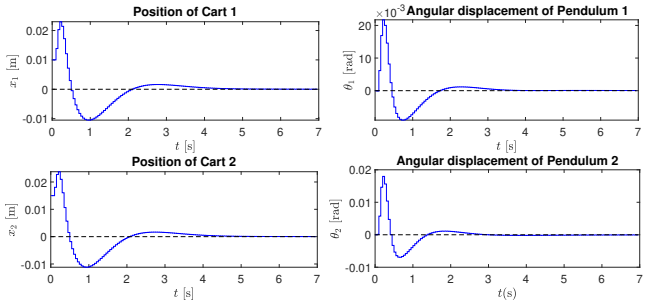

Fig. 2. System outputs based on state feedback offset-free predictive control of the parallel type double inverted pendulum for initial condition $\bar{x}$.

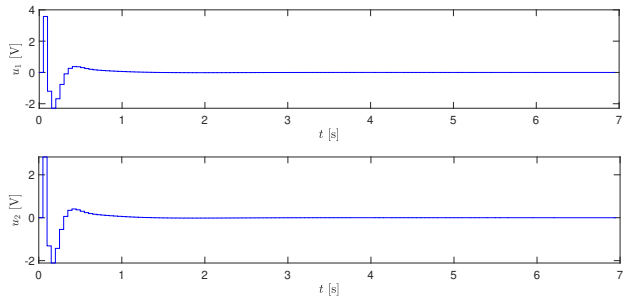

Fig. 3. Control signals for state feedback offset-free predictive control of the parallel type double inverted pendulum for initial condition $\bar{x}$.

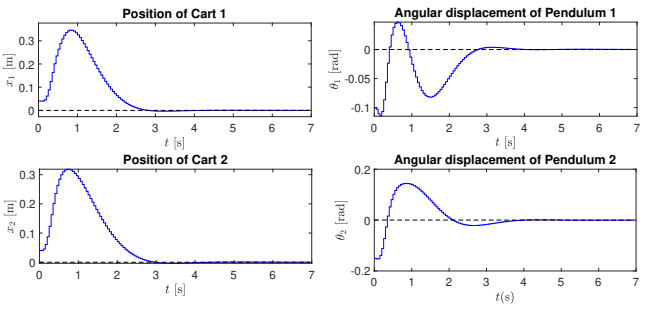

Fig. 4. System outputs based on state feedback offset-free predictive control of the parallel type double inverted pendulum for initial condition $\bar{\bar{x}}$.

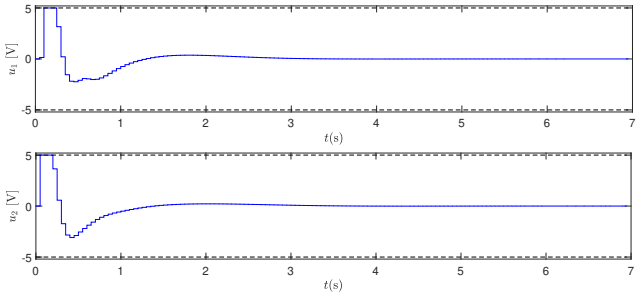

Fig. 5. Control signals for state feedback offset-free predictive control of the parallel type double inverted pendulum for initial condition $\bar{\bar{x}}$. Dash line indicates voltage constraints.

carts positions and pendulums angles deviate from the equilibrium to test the robustness of the controller to modelling errors (due to linearity assumptions). The initial condition which is chosen as $\bar{\bar{x}} = [0.04, -0.1, 0.04, -0.15, 0, 0, 0, 0]^T$ can also be used to comment on the ability of the controller to handle saturation of the input signal. The plots obtained for the outputs are shown in Figure 4 and the control signals are demonstrated in Figure 5.

B. Observer-based Control

To implement an observer-based OfMPC scheme, it is assumed that only the outputs of the system are measurable which means that the velocities of the carts and pendulums angles need to be estimated. To achieve the estimation of the unmeasured states, Kalman filtering is used. To implement the observer, process weight matrix is selected as $Q_n = I_{8\times 8}$ while the output weighting matrix $R_n = I_{4\times 4}$. Thus, the observer gain is obtained as:

$$L = \begin{bmatrix} 0.3097 & 0.0304 & 0.0069 & -0.0272 \\ 0.0633 & 0.4900 & -0.0609 & -0.0018 \\ 0.0069 & -0.0272 & 0.3097 & 0.0304 \\ -0.0609 & -0.0018 & 0.0633 & 0.4900 \\ 0.2495 & 0.0553 & 0.0143 & -0.0219 \\ 0.8542 & 1.7002 & -0.8407 & 0.0719 \\ 0.0143 & -0.0219 & 0.2495 & 0.0553 \\ -0.8407 & 0.0719 & 0.8542 & 1.7002 \end{bmatrix} \tag{25}$$

Just like in the state feedback scenario, the system is simulated under two different initial conditions using the same controller settings. Since it is almost unavoidable for measurement noise to impact the measured variables, white Gaussian noise with signal-to-noise ratio of 35dB is added to

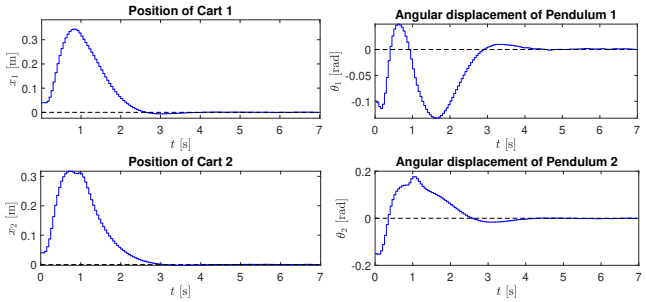

Fig. 8. System outputs for the observer-based offset-free predictive control of the parallel type double inverted pendulum for initial condition $\bar{\bar{x}}$.

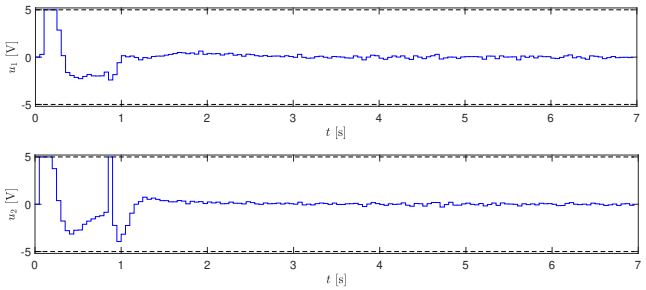

Fig. 9. Control signals for the observer-based OfMPC. Dash line indicates voltage constraints.

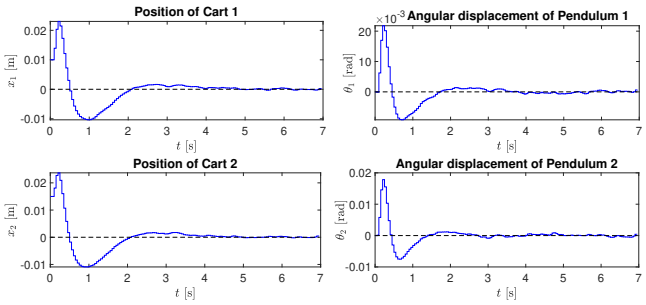

Fig. 6. System outputs for the observer-based offset-free predictive control of the parallel type double inverted pendulum for initial condition $\bar{x}$.

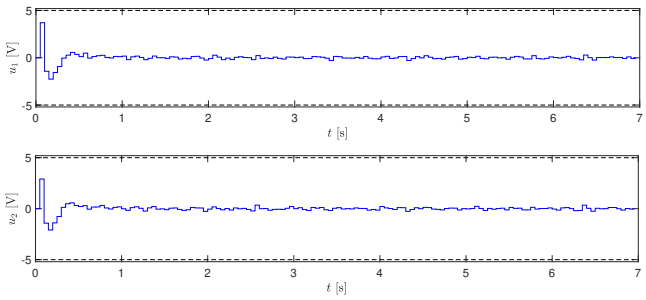

Fig. 7. Control signals for the observer-based OfMPC. Dash line indicates voltage constraints.

the measured outputs. The results obtain for the initial system conditions of $\bar{x}$ is shown in Figure 6 and 7, where the outputs and control voltages are shown respectively. Furthermore, the simulation results for the system under the initial condition $\bar{\bar{x}}$ are presented in Figures 8 and 9.

V. Discussion of Results

The numerical simulation presented in the previous section considered two scenarios. The first scenario represents the ideal case where all the states are assumed to be measurable in order to be able to implement the OfMPC which is traditionally a state feedback controller. However, in practice, it is not desirable to measure all the states of the system both from the economic and weight implications on the system as well as the simplicity of the implementation of the controller. Hence, the second scenario assumed that only the outputs - the carts displacements and angular position, needs to be measured which made it necessary to estimate four additional states based on Kalman filtering. Since measurements are usually affected by noise, white Gaussian noise was assumed to affect the measurements used to implement the observer-based OfMPC. The results show that for initial conditions of the system with minimal deviations from the equilibrium points of the system such as $\bar{x}$, the proposed OfMPC is able to stabilize the system in less than 5 s while ensuring that the physical constraints conditions are met. This is clear from Figures 2 and 6 where the carts positions x_1 and x_2 lie with $\pm$1m while the control signal stayed with $\pm$5V in Figures 3 and 7. Besides, the stabilisation of the system was also achieved in less than 5s even when the more challenging initial state $\bar{\bar{x}}$ was employed in the simulations. Therefore, the proposed OfMPC can drive the system states to the equilibrium states from deviations not too far from the linearization points in less than 5 seconds.

VI. Conclusions

This paper presented a nonlinear model of the parallel-type double inverted pendulum system based on the Lagrange equation. To achieve a stabilising control of the developed nonlinear model, a linear OfMPC was developed and its effectiveness was verified in the presence of input and state constraints under two conditions. The first condition assumes that all the system states are measurable which may not be desirable in practical applications. The second condition which is formulated to mimic the practical implementation assumes that only the outputs are measurable and that the measurements are affected by white Gaussian noise. Future research works may consider experimental validation of the method by comparing it with the LQR controller which was proposed in previous studies. Moreover, the model can be useful for testing and validating novel control methods. Furthermore, future research may also investigate swing-up control for the system.

References

[1] S.-J. Huang and C.-L. Huang, "Control of an inverted pendulum using grey prediction model," *IEEE transactions on industry applications*, vol. 36, no. 2, pp. 452–458, 2000.

[2] H. Gao, X. Li, C. Gao, and J. Wu, "Neural network supervision control strategy for inverted pendulum tracking control," *Discrete Dynamics in Nature and Society*, vol. 2021, 2021.

[3] M. Waszak and R. Łangowski, "An automatic self-tuning control system design for an inverted pendulum," *IEEE Access*, vol. 8, pp. 26 726–26 738, 2020.

[4] A. Voevoda, A. Koryukin, and A. Chekhonadskikh, "Reducing the stabilizing control order for a double inverted pendulum," *Optoelectronics, instrumentation and data processing*, vol. 48, no. 6, pp. 593–604, 2012.

[5] T. M. Tijani and I. A. Jimoh, "Optimal control of the double inverted pendulum on a cart: A comparative study of explicit MPC and LQR," *Applications of Modelling and Simulation*, vol. 5, pp. 74–87, 2021.

[6] S. Jadlovská and J. Sarnovskỳ, "Classical double inverted pendulum—a complex overview of a system," in *2012 IEEE 10th International Symposium on Applied Machine Intelligence and Informatics (SAMI)*. IEEE, 2012, pp. 103–108.

[7] A. D. Kuo, "The six determinants of gait and the inverted pendulum analogy: A dynamic walking perspective," *Human movement science*, vol. 26, no. 4, pp. 617–656, 2007.

[8] T. Sugihara, Y. Nakamura, and H. Inoue, "Real-time humanoid motion generation through zmp manipulation based on inverted pendulum control," in *Proceedings 2002 IEEE International Conference on Robotics and Automation (Cat. No. 02CH37292)*, vol. 2. IEEE, 2002, pp. 1404–1409.

[9] R. Altendorfer, U. Saranli, H. Komsuoglu, D. Koditschek, H. B. Brown, M. Buehler, N. Moore, D. McMordie, and R. Full, "Evidence for spring loaded inverted pendulum running in a hexapod robot," *Experimental Robotics VII*, pp. 291–302, 2001.

[10] J. Yi, N. Yubazaki, and K. Hirota, "A new fuzzy controller for stabilization of parallel-type double inverted pendulum system," *Fuzzy Sets and Systems*, vol. 126, no. 1, pp. 105–119, 2002.

[11] O. Gonzalez and A. Rossiter, "Fast hybrid dual mode NMPC for a parallel double inverted pendulum with experimental validation," *IET Control Theory & Applications*, vol. 14, no. 16, pp. 2329–2338, 2020.

[12] J. Yi, N. Yubazaki, and K. Hirota, "Stabilization fuzzy control of parallel-type double inverted pendulum system," in *Ninth IEEE International Conference on Fuzzy Systems. FUZZ-IEEE 2000 (Cat. No. 00CH37063)*, vol. 2. IEEE, 2000, pp. 817–822.

[13] D. Zhu and D. Zhou, "Synchronization control of parallel dual inverted pendulums," in *2008 IEEE International Conference on Automation and Logistics*. IEEE, 2008, pp. 1486–1490.

[14] L. Xing, Y. Chen, and X. Wu, "A novel parallel-type double inverted pendulum control method," in *2010 IEEE International Conference on Intelligent Computing and Intelligent Systems*, vol. 1. IEEE, 2010, pp. 880–887.

[15] I. A. Jimoh, I. B. Küçükdemiral, and G. Bevan, "Fin control for ship roll motion stabilisation based on observer enhanced MPC with disturbance rate compensation," *Ocean Engineering*, vol. 224, p. 108706, 2021.

[16] J. H. Lee, "Model predictive control: Review of the three decades of development," *International Journal of Control, Automation and Systems*, vol. 9, no. 3, pp. 415–424, 2011.

[17] D. Limón, I. Alvarado, T. Alamo, and E. F. Camacho, "MPC for tracking piecewise constant references for constrained linear systems," *Automatica*, vol. 44, no. 9, pp. 2382–2387, 2008.

[18] A. H. González, E. J. Adam, and J. L. Marchetti, "Conditions for offset elimination in state space receding horizon controllers: A tutorial analysis," *Chemical Engineering and Processing: Process Intensification*, vol. 47, no. 12, pp. 2184–2194, 2008.

[19] I. A. Jimoh, I. B. Küçükdemiral, G. Bevan, and P. E. Orukpe, "Offset-free model predictive control: A study of different formulations with further results," in *2020 28th Mediterranean Conference on Control and Automation (MED)*. IEEE, 2020, pp. 671–676.

[20] J. Fan, X. Wang, and M. Fei, "Research of parallel-type double inverted pendulum model based on lagrange equation and LQR controller," in *Life System Modeling and Intelligent Computing*. Springer, 2010, pp. 147–156.

[21] L. Yue-song, Q. Ji-xin, X. An-ke, and W. Jun-Hong, "Simple multi-pd control algorithm of double inverted pendulum," in *2002 IEEE Region 10 Conference on Computers, Communications, Control and Power Engineering. TENCOM'02. Proceedings.*, vol. 3. IEEE, 2002, pp. 1428–1431.

[22] D. L. Di Ruscio, "Model predictive control with integral action: a simple mpc algorithm," *Modeling, Identification and Control*, vol. 34, no. 3, pp. 119–129, 2013.

[23] I. B. Kucukdemiral, F. Cakici, and H. Yazici, "A model predictive vertical motion control of a passenger ship," *Ocean Engineering*, vol. 186, p. 106100, 2019.

[24] I. A. Jimoh, "A novel approach to disturbance rejection in constrained model predictive control," *Master of Science Thesis, Glasgow Caledonian University. Available as arXiv preprint arXiv:2103.09865*, 2021.

[25] D. Q. Mayne, "Model predictive control: Recent developments and future promise," *Automatica*, vol. 50, no. 12, pp. 2967–2986, 2014.